



UNIVERSITY OF LEEDS

This is a repository copy of *Defect-mediated CO₂ activation at two-dimensional MgO monolayers: A DFT study*.

White Rose Research Online URL for this paper:

<https://eprints.whiterose.ac.uk/id/eprint/227290/>

Version: Accepted Version

Article:

Kumar, K., Dhasmana, A., Mishra, S. et al. (4 more authors) (2025) Defect-mediated CO₂ activation at two-dimensional MgO monolayers: A DFT study. *Materials Today Communications*, 46. 112907. ISSN 2352-4928

<https://doi.org/10.1016/j.mtcomm.2025.112907>

This is an author produced version of an article published in *Materials Today Communications*, made available under the terms of the Creative Commons Attribution License (CC-BY), which permits unrestricted use, distribution and reproduction in any medium, provided the original work is properly cited.

Reuse

This article is distributed under the terms of the Creative Commons Attribution (CC BY) licence. This licence allows you to distribute, remix, tweak, and build upon the work, even commercially, as long as you credit the authors for the original work. More information and the full terms of the licence here:

<https://creativecommons.org/licenses/>

Takedown

If you consider content in White Rose Research Online to be in breach of UK law, please notify us by emailing eprints@whiterose.ac.uk including the URL of the record and the reason for the withdrawal request.



eprints@whiterose.ac.uk
<https://eprints.whiterose.ac.uk/>

Defect-mediated CO₂ activation at two-dimensional MgO monolayers: A DFT study

Kamal Kumar¹, Abhishek Dhasmana¹, Soni Mishra², Ramesh Sharma³, Nora H. de Leeuw^{4,5},
Jost Adam^{6,7}, Abhishek K. Mishra^{1*}

¹Department of Physics, Applied Science Cluster, UPES, Dehradun, Uttarakhand 248007, India

²Department of Physics, Graphic Era Hill University, Dehradun 248002, India

³Department of Applied Science, Feroze Gandhi Institute of Engineering and Technology,
Raebareli, 229001, Uttar Pradesh, India

⁴School of Chemistry, University of Leeds, Leeds LS2 9JT, UK

⁵Department of Earth Sciences, Utrecht University, 3584 CB Utrecht, The Netherlands

⁶Computational Materials and Photonics, Department of Electrical Engineering and Computer
Science (FB 16) and Institute of Physics (FB 10), University of Kassel, Wilhelmshoher Allee 71,
34121 Kassel, Germany

⁷Center for Interdisciplinary Nanostructure Science and Technology, University of Kassel,
Heinrich-Plett-Straße 40, 34132 Kassel, Germany

ABSTRACT

CO₂ capture is vital to address fossil fuel depletion and to mitigate climate change by reducing the emission of greenhouse gases and fostering the sustainable generation and use of energy. Through first-principles calculations based on the density functional theory (DFT), in this work we report the CO₂ adsorption characteristics at graphene-like pristine and defect-containing 2-dimensional MgO monolayers via a detailed investigation of the electronic and geometrical changes. Mono-vacancy, di-vacancy (O and Mg atoms vacancies), and anti-site defects (MgO_{-A}) are studied and our results show chemisorption of the CO₂ molecule at 2D MgO with an adsorption energy of -0.79 eV and bending of its linear geometry. Introducing O and Mg vacancies leads to an increase of about 80% and 178%, respectively, in these adsorption energies. The anti-site defect MgO_{-AMg} (O atom replaced by Mg atom) was found to be thermodynamically unfavorable, as indicated by a calculated positive defect formation energy, while all other defects exhibit negative formation energies. In the present work, we found that activation of the CO₂ molecule occurs at all considered MgO sheets. Engineered atomic defects increase this process, with a maximum adsorption energy of -3.97 eV at the MgO_{-Mg/O} sheet, containing both Mg and O atom vacancies. The defect creation and interaction between the 2D MgO monolayer and CO₂ molecule alters the distribution of atomic orbitals as confirmed through projected density of states (PDOS), which is indicative of CO₂ activation on these MgO 2d sheets.

* Corresponding author email id: mishra_lu@hotmail.com; akmishra@ddn.upes.ac.in

Keywords: 2D MgO, CO₂ activation, Defects, DFT

1. Introduction

Two-dimensional (2D) metal oxides (MOs) have earned significant interest owing to their fascinating properties [1]. Recently, various planar hexagonal metal oxide layers have been predicted and synthesized, which are different from their traditional non-planar geometrical arrangements [2]. This unique family of 2D nanomaterials includes a wide range of experimentally synthesized materials, including alkaline metal oxides, alkaline earth metal oxides and transition metal oxides [1]. Furthermore, 2D MOs possess a plethora of applications, e.g. as super-capacitors, gas sensors, photo-catalysts, in lithium and hydrogen storage, spintronics, piezoelectricity, energy storage and optoelectronics [1].

Zheng *et al.* theoretically predicted the graphene-like hexagonal and planar 2D monolayer of MgO (see **Figure 1(a), (b)**) and confirmed its semiconducting nature with an indirect band gap and good dynamical stability[3]. Following theoretical predictions, researchers managed to synthesize 2D MgO, where porous 2D MgO nanosheets were prepared by precipitation of magnesium nitrate using ammonium carbonate as a precipitating agent[4]. Compared to commercial MgO, this highly porous material was effective at adsorbing phosphate, removing 95% of the particle with a removal capacity of 255.1 mg g⁻¹. Because of its high phosphate adsorption efficiency, magnesium oxide nanosheets are a desirable adsorbent in water remediation, helping to solve long-term issues[4]. Hoat *et al.* studied the effect of functionalization (N and F) on the structural, electronic, and optical characteristics of 2D MgO monolayers and found that surface functionalization induces a buckling of the planar MgO monolayer, allowing MgO monolayers to adsorb light over a wide range of wavelengths (infrared to ultraviolet), which suggests that the functionalized MgO monolayers could be employed in optoelectronic devices, including sensors and photovoltaic cells[5]. Moghadam *et al.* studied the optical and magnetic properties of F, N, C, and B-doped MgO monolayers and found that the doping by single F, C, and N atoms generates magnetization in MgO monolayers, resulting in magnetic and half-metallic behaviour, while doping by single F atoms promotes non-magnetic characteristics, which indicates its potential applications in spintronic devices where magnetic properties can be precisely controlled by doping[6]. Moreover, the high thermal stability of the 2D MgO monolayer makes it a promising candidate for high-temperature applications. Its basic nature allows it to interact favourably with acidic gases, making it useful for environmental applications such as CO₂ capture and conversion[5–7]. Additionally,

the high reactivity and semiconducting properties make 2D MgO attractive for catalysis and in electronic devices[8,9].

Defect engineering is a powerful technique to tune the surface chemistry and chemical activity of MOs, specifically in the context of CO₂ adsorption and activation [10]. In general, pristine MOs achieve low adsorption energies and are unable to activate CO₂ for further conversion [11]. However, the creation of defects and vacancies significantly changes the distribution of electronic states [11]. Vacancies generate localized states in the band gap and create dangling bonds [12]. These defect sites promote strong hybridization between the surface of the MO and adsorbed CO₂ molecules [11,12]. In addition, localized lone pairs caused by defects can interact with the C atom of the CO₂ molecule which leads to weakening of the C=O bond and bending of the linear CO₂ geometry [10]. The surface of MgO is rich in defects, featuring point defects (mono-vacancies, di-vacancies) and line defects [13,14], which can serve as holes and electrons traps at the surface. Several studies are available in the literature that are focused on exploring the effect of defects on various properties of the MgO surface, as well as 2D MgO sheets [13–15]. Baranek *et al.* theoretically characterized a V centre in the bulk and (001) surface of MgO [15] and showed that migration is more favourable at the (001) surface [15].

Lv *et al.* have employed first-principles based density functional theory calculations to investigate the CO₂ adsorption mechanism at two (Mg-O) sites generated by calcination of Mg-Al-CO₃ layered double hydroxides (LDH) into layered double oxides (LDO) [16]. Their study revealed that among various MgO surfaces, including (110), (100), (111), (210) and (211), the MgO (100) surface is the most stable surface and exhibits the smallest surface energy (1.30 J/m²)[16]. They found that doping by Al atoms and the creation of vacancy defects in the Mg (100) surface enhances its CO₂ adsorption capacity. The calculated adsorption energy of CO₂ at the Al-doped MgO (110) surface was -1.05 eV which was 0.73 eV higher than at the pristine MgO (110) surface, while vacancy creation increased the adsorption energy up to -1.96 eV [16]. Cornu *et al.* used DFT calculations to study CO₂ adsorption at defects (corners, kinks, steps and di-vacancy) in the MgO (100) surface and reported high adsorption energies for the CO₂ molecule at corner (-1.53 eV), kink (-2.02 eV), step (-2.26 eV) and di-vacancy (-1.97 eV) sites in the MgO (100) surface[17]. Apart from CO₂ adsorption, MgO can be applied in different domains, including medical (cancer treatments and antiseptic), environmental (clean energy production, waste water treatment, antibacterial activities) electronics (low magnetic field sensors, insulation and resistive switching)

and spintronics applications [18]. A DFT study by On *et al.* found that 2D MgO with Mg vacancies is ferromagnetic, while 2D MgO with O vacancies and a combination of both O and Mg vacancies is paramagnetic. Thus, 2D MgO with Mg vacancies is a promising material for spin-filtering applications[19]. Hazarika *et al.* studied the optoelectronic properties of defect-containing (O-vacancy) MgO monolayers using DFT. Their study reveals that the creation of an O-vacancy causes a red shift in different optical phenomena. MgO monolayers with di-vacancies possess maximum optical absorption and show optical activity from the visible to ultraviolet range of the electromagnetic spectrum. As such, 2D MgO with vacancies is suitable in the design of effective materials for solar energy applications[20]. Thus, while the presence of vacancies and defects has been explored for spin-filtering and solar energy applications, the activation or reduction of CO₂ on pristine as well as defect-containing 2D MgO monolayer has not as yet been studied.

In this work, we have employed first-principles based DFT calculations to investigate the formation of defects in 2D MgO and the interaction of CO₂ molecules with the pristine and defect-containing 2D MgO monolayers. For defect-containing 2D MgO, we have considered mono-vacancies (one oxygen atom is missing MgO-O; one Mg atom is missing MgO-Mg), di-vacancies (one O and one Mg are missing MgO-Mg/O), and anti-site defects (MgO-A). The interaction, nature, and strength of adsorption on these systems are confirmed through projected density of states (PDOS), electronic band structure (EBS), and Bader charge transfer calculations and charge density difference plots.

2. Computational Details

We have employed the Quantum Espresso (QE) code, an open-source software package, within the framework of DFT[21], for the present calculations. For the precision in the calculations of the electronic structure through the variation in electron density, the Perdew-Burke-Ernzerhof (PBE) functional was adopted in its gradient corrected form[22,23]. The projected augmented wave method (PAW) was used to treat the interactions between electrons and ions[24]. The Grimme-d3 approach for the Van der Waals correction was further employed to consider long-range interactions[25]. In order to investigate defects and CO₂ interaction, a 4×4 supercell of a free-standing 2D MgO monolayer was modelled, containing 16 magnesium (Mg) and 16 oxygen (O) atoms (**Figure 2(a)**). The interactions between adjacent cells were eliminated by introducing a vacuum of 10 Å along the z-direction or perpendicular to the 2D MgO plane. Monkhorst-Pack k-

point grids of $5 \times 5 \times 1$ for ground state energy calculations and $10 \times 10 \times 1$ for density of states calculations were used to sample the Brillouin zone integration. A well-converged cut-off kinetic energy of 60 Ry was employed.

The defect formation energy (E_{def}) and adsorption energy (E_{ads}) of CO_2 were determined through equations (1) and (2), respectively.

$$E_{\text{def}} = E_{\text{MgO}} - (E_{\text{MgO}_{\text{vac}}} + E_X), \quad (1)$$

$$E_{\text{ads}} = E_{\text{sheet}+\text{CO}_2} - (E_{\text{sheet}} + E_{\text{CO}_2}), \quad (2)$$

where E_{MgO} and $E_{\text{MgO}_{\text{vac}}}$ are the total energies of the pristine and vacancy-containing 2D MgO, while E_X ($X=\text{O}, \text{Mg}$) is the total energy of the removed atoms for which we seek to determine E_{def} . $E_{\text{sheet}+\text{CO}_2}$ and E_{CO_2} are the total energies of the CO_2 -adsorbed 2D MgO sheet and the isolated CO_2 molecule, respectively. E_{sheet} is the system's total energy for which we need to calculate the E_{ads} of the CO_2 molecule. The Gibbs free energy (ΔG) was calculated by equation (3)

$$\Delta G = E_{\text{ads}} + \Delta \text{ZPE} - T\Delta S \quad (3)$$

Where, ΔG , ΔZPE , T and ΔS are the Gibbs free energy, change in zero-point energy of the CO_2 molecule, temperature and change in entropy, respectively. Since our adsorption energy calculations are carried out at absolute zero temperature (0 K) which is the standard approach in DFT studies, the third term ($T\Delta S$) in equation (3) vanishes.

3. Results and discussion

3.1 Structural and Electronic properties

3.1.1 Pristine 2D MgO Monolayer sheet

The geometrical structure of a 2D MgO monolayer resembles a flat hexagonal honeycomb lattice similar to a graphene nanosheet. Its unit cell (as shown in the black ellipse in **Figure 1 (a)**) consists of one magnesium (Mg) and one oxygen atom (O) and belongs to the $P6m2$ space group (no. 187). **Figure 1(a)** shows the arrangement of Mg and O atoms in a 4×4 supercell of the 2D MgO monolayer. Our calculated lattice parameter for a 2D MgO unit cell was found to be 3.30 \AA and is in agreement with earlier works[5]. After optimization, the interatomic bond angle and bond lengths of Mg and O atoms are found to be 120.01° and 1.90 \AA , respectively, reflecting the planar lattice structure of the 2D MgO monolayer (see **Table 1**).

Table 1 :

Optimized lattice constant a , b (Å), bond length l (Å) and bond angle θ (°) of the 2D MgO monolayer unit cell and comparison with earlier DFT works.

Lattice constants, geometrical parameters	Our Work	Earlier DFT Works			
		Hoat et al. [5]	Van et al.[26]	Alyoruk et al.[27]	Zheng et al.[3]
a	3.30	3.29	3.30	3.30	3.24
b	3.30	3.29	3.30	3.30	3.24
l (Mg-O)	1.90	1.90	1.91	-----	1.87
θ	120.01	120	-----	-----	-----

In order to understand the electrical properties of 2D MgO monolayers, we have plotted their projected electronic density-of-states (PDOS) and electronic band structure (EBS) in **Figures 1(c)** and **1(d)**, respectively. The 2D MgO monolayer has an indirect band gap (E_g) of 2.81 eV, where the top of the valence band (VB) is found to be located at the K symmetry point, while the bottom of the conduction band (CB) is found at the Γ high symmetry point in the EBS. Our PDOS and EBS of pristine MgO possess a similar nature when compared to earlier works of Hoat et al. [5]. Since the electronegativity of the Mg atom is less than that of the O atom, this difference in electronegativity is responsible for the transfer of two electrons from the outer s-orbital of the Mg atom to the outermost p-subshell of the O atom. After donating two electrons, the Mg atom contains vacant 3s and 3p orbitals, while the 2p orbital of the O atom is filled by the extra electrons from the Mg atom. As such, in the PDOS of the 2D MgO monolayer, the s-orbital contributes in the lower region of the CB, and the p-orbital of the O atom dominates in the upper part of the VB. As a result, the bonding between Mg and O in the 2D MgO monolayer is ionic, along with minimal overlapping of the atomic orbitals.

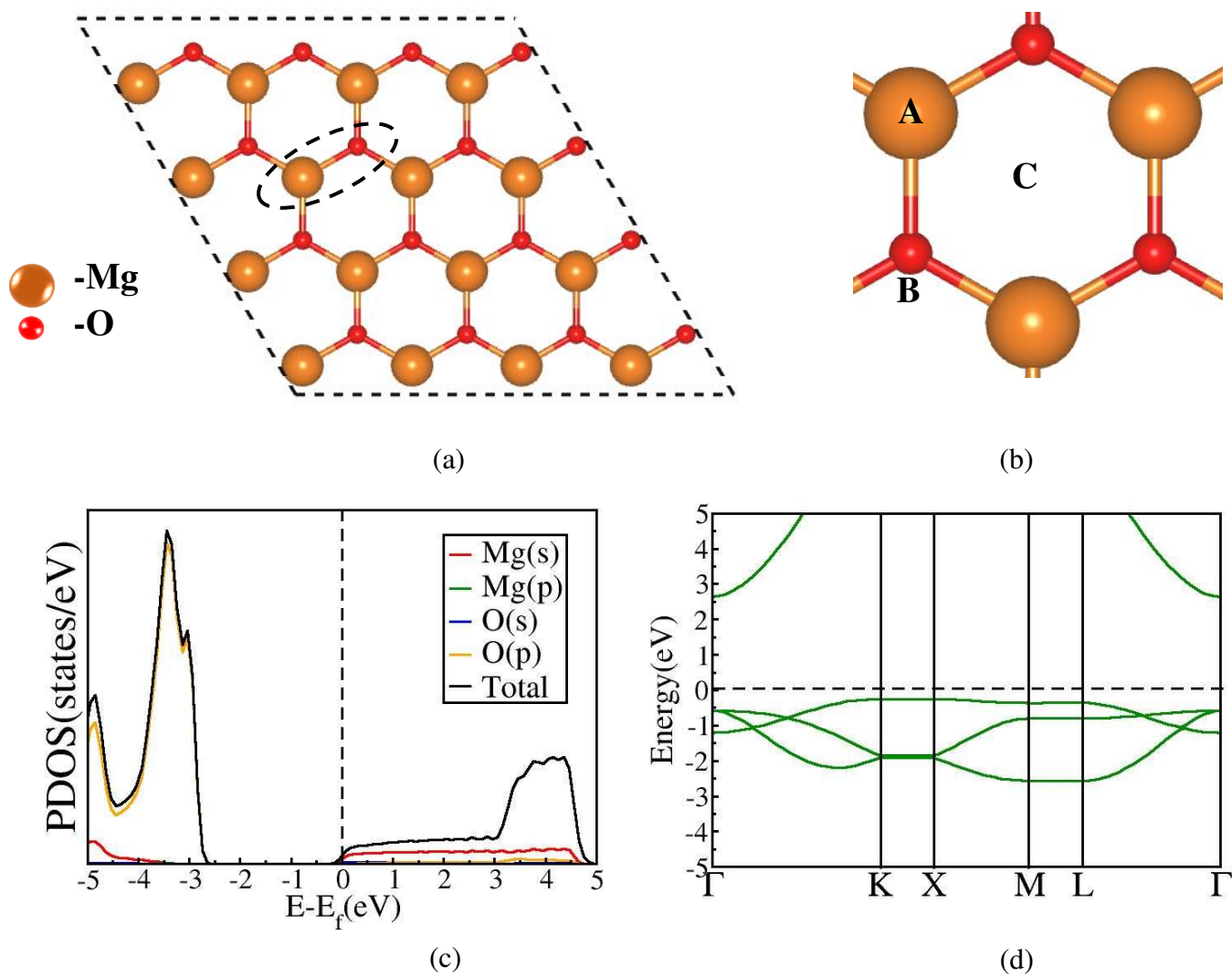


Fig. 1. (a) Optimized 4×4 2D MgO supercell, (b) investigated CO₂ adsorption sites on 2D MgO (c), and (d) PDOS and EBS of the 2D MgO respectively. Orange and red colors represent magnesium and oxygen atoms, respectively. The maximum contribution in valance band arises from p-orbital of O atom.

3.1.2 Defect-containing 2D MgO monolayer sheets

As discussed in the *Introduction* section, for a more realistic representation of experimental 2D MgO sheets, we have introduced a number of vacancy defects, both mono- and di-vacancies, as

shown in **Figure 2(a)-(f)**. First, we removed a single O atom from our 4×4 supercell model (**Figure 2(b)**) and calculated the defect formation energy (E_{def}), using expression (1), to be -10.04 eV. A comparison with a similar DFT study by Bafekry *et al.* of pristine and defect-containing BeO monolayers revealed that the E_{def} for the O atom in the BeO monolayer was found to be -7.30 eV[28], indicating more susceptibility of the 2D MgO layer towards an O atom vacancy compared to a 2D BeO monolayer. The effect of vacancies on the electrical properties was also investigated, and as expected, the presence of the O-vacancy decreases the band gap to 1.29 from its original value of 2.29 eV, while its nature remains indirect (**Figure 4**). The nearby Mg-O bond lengths of $\text{MgO}_{-\text{O}}$ were found to be almost the same as in pristine MgO sheets, which implies that $\text{MgO}_{-\text{O}}$ has a stable geometrical structure without any significant local strain.

The defect formation energy for a single Mg vacancy ($\text{MgO}_{-\text{Mg}}$) was calculated to be -10.51 eV, which is almost same as was calculated for the O vacancy. As a result of the Mg vacancy in the MgO monolayer (**Figure 2(c)**), the bond strength of Mg-O atoms increases at the defect site as the Mg-O bond length contracts from 1.90 Å to 1.87 Å. Here, we note only a slight decrease in the band gap which was found to be 2.24 eV (**Figure 4**). In both types of vacancies the major contribution in PDOS arises from the p-orbital of the O atoms.

Next, we investigated the di-vacancy formation by removing one Mg and one O atom in a MgO 2D sheet (**Figure 2(d)**). We found these defects to be more favourable with a calculated defect formation energy to be -16.87 eV. The creation of this di-vacancy contracts the Mg-O bond lengths by up to 3.68% due to redistribution of the atom positions. This $\text{MgO}_{-\text{Mg/O}}$ system is a narrow band gap semiconductor with an indirect band gap of 0.70 eV (**Figure 4**).

We have also investigated anti-site defects by replacing one Mg atom with one O atom and found the defect formation energy corresponding to this added O atom to be -5.65 eV for the $\text{MgO}_{-\text{AO}}$ sheet, while replacing one O atom with an Mg atom (**Figure 2(e)**) results in a positive defect formation energy of 3.50 eV. This was expected due to the ionic size mismatch of Mg^{2+} (0.72 Å) and O^{2-} (1.40 Å) whereas swapping the cation and anion disrupts the electrostatic stability of the system. The obtained O-O bond length in the $\text{MgO}_{-\text{AO}}$ sheet after relaxation was 1.80 Å, while nearby Mg-O bond lengths expanded to 1.93 Å, indicating weaker bond strengths than in the pristine or single atom vacancy sheets of MgO. The band gap of $\text{MgO}_{-\text{AO}}$ was found to be 1.0 eV, (**Figure 4**) along with a direct transition of an electron from VB to CB at high symmetry point X.

As mentioned, the formation of MgO-AMg systems is not spontaneous, and it requires external energy to bind additional Mg atoms in its lattice. The presence of this Mg atom decreases the separation between the energy band and transforms the 2D MgO monolayer from an indirect to a direct band gap semiconductor. After geometry optimization, the optimized Mg-Mg and Mg-O bond lengths of an MgO-AMg system were found to be 2.61 Å and 1.83 Å respectively.

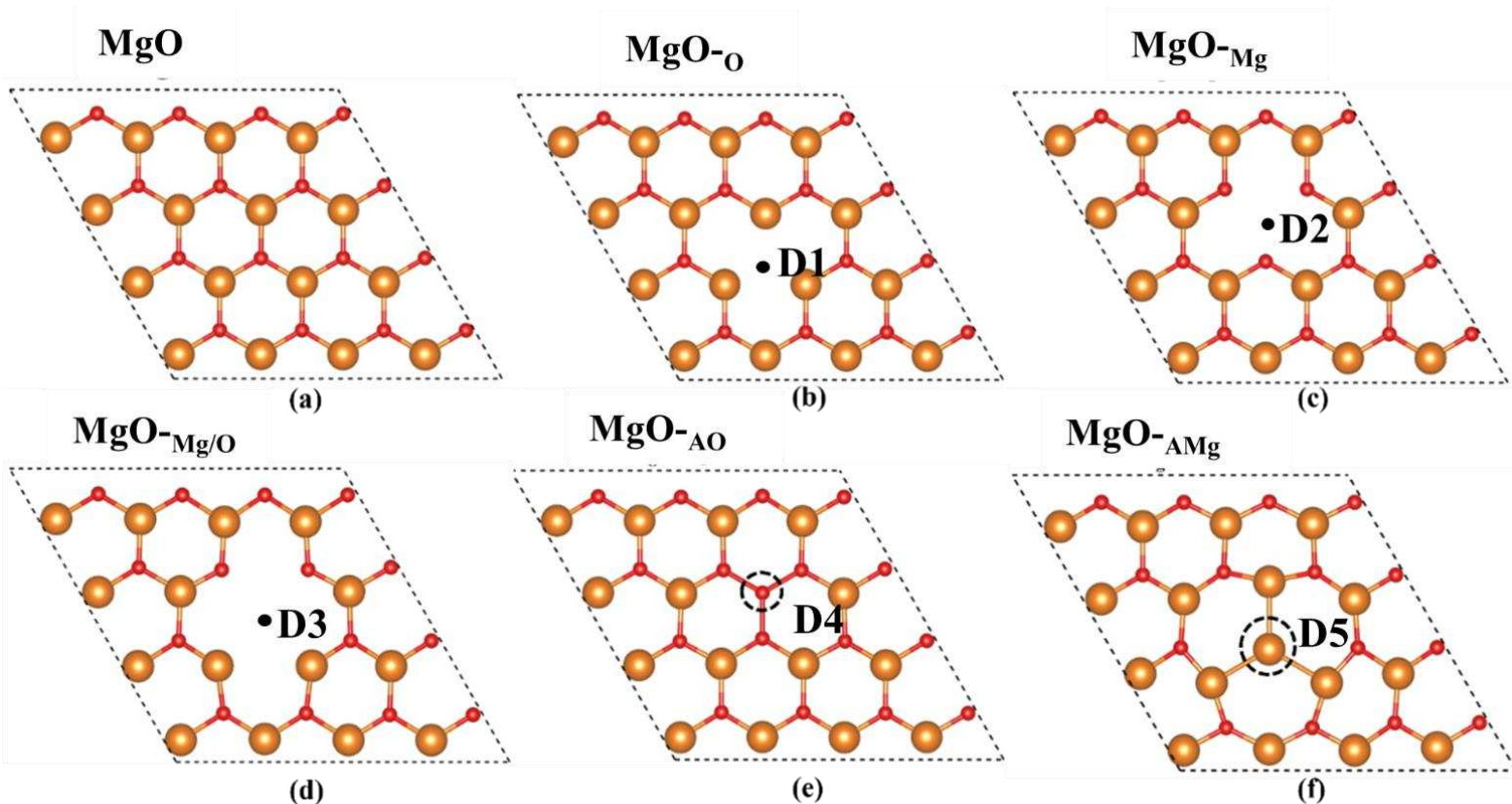


Fig. 2. Optimized structure of (a)MgO, (b) MgO-O, (c) MgO-Mg, (d) MgO-Mg/O, (e) MgO-AO, and (f) MgO-AMg sheets

3.2 CO₂ activation characteristics

3.2.1 Pristine 2D MgO monolayer sheet (CO₂@MgO)

In this section, we present and discuss the activation of CO₂ molecules on a pristine 2D MgO monolayer sheet (MgO). Considering the crystallographic symmetry of 2D MgO, we identified three adsorption sites for CO₂ as follows: A-site (above Mg-atom), B-site (above O-atom), and C-site (center of the hexagonal ring) (see **Figure 1(b)**). The CO₂ molecule was placed at these sites

in both vertical/perpendicular (\perp) and horizontal/parallel (\parallel) configurations, and we also tried a few inclined configurations at the bridge site between the Mg and O atoms. We have given the six different configurations of the CO₂ molecule interacting with the MgO monolayer in **Figure S2** along with their calculated adsorption energies E_{ads} and geometrical parameters in **Table S1**. We note that the CO₂ molecule binds with the pristine MgO sheet at a height of 1.35 Å with an adsorption energy of -0.79 eV, as shown in **Figure 3**. Here, the CO₂ molecule bends to an $\angle\text{OCO}$ of 130.51°, while the O-C bonds are found to be 1.26 Å. The most stable arrangement occurred when the CO₂ molecule was placed parallel to the 2D MgO in such a fashion that the C atom of the CO₂ molecule was positioned above the O atom of 2D MgO (second configuration of **Table S1**). Thus, the B-site in the \parallel configuration is the most active site for the CO₂ molecule on MgO with an E_{ads} of -0.79 eV surpassing -0.14 eV, the threshold value for practical applications [29]. After relaxation, one of the C-O bonds of the CO₂ molecule elongated to 1.26 Å, and the CO₂ molecule lost its linear geometry as the molecule bent to 130.51°. Due to the high E_{ads} and structural modification of the CO₂ molecules, the adsorption of CO₂ on 2D MgO can be classified as chemisorption. This adsorption of CO₂ on a graphene-like 2D MgO monolayer is stronger than the adsorption reported by Wang *et al.* for a graphene sheet (weak physisorption with E_{ads} of -0.23 eV for pristine graphene)[30]. We further analyzed the interaction of the CO₂ molecule with this 2D MgO sheet through molecular orbital interaction investigated through PDOS plots. We note that as a result of the interaction, the band gap of 2D MgO changes significantly as the value of band gap, E_g , reduces to 2.29 eV after CO₂ adsorption. This interaction also disturbs the distribution of the energy levels in EBS, and the nature of the band gap changes to direct from its indirect band gap nature. This activation of CO₂ leads to the origin of a new peak near -3 eV in the conduction band due to the p-orbital of a CO₂ molecule's carbon atom. The Bader charge analysis suggests charge transfer of 0.02e⁻ between the CO₂ molecule and 2D MgO sheet.

3.2.2 Defect-containing 2D MgO monolayer sheets

Defects are electron trap sites and the presence of atomic and molecular defects are primarily responsible for the improved CO₂ adsorption by causing localized electronic states and unsaturated coordination sites. We investigated the effect of defects on the interaction between various defect-containing 2D-MgO monolayer sheets and the CO₂ molecule, except for the MgO-

$_{AMg}$ system because of its thermodynamically instability as calculated through the defect formation energy values. We considered different sites as marked in **Figure 2** for the various vacancy-containing 2D MgO sheets, i.e. D1 (MgO- $_O$), D2(MgO- $_{Mg}$), D3(MgO- $_{Mg/O}$), D4(MgO- $_{AO}$) and D5(MgO- $_{AMg}$).

As mentioned, first in order to explore the influence of an O-vacancy in the 2D MgO monolayer (MgO- $_O$) on the CO₂ adsorption characteristics, different configurations were investigated near the vacancy site (site D1 in **Figure 2**). All the studied configurations of CO₂ at the MgO- $_O$ sheet are given in **Figure S4** of the supplementary information and the obtained E_{ads} , along with structural parameters, are summarized in **Table S2**. A few of the considered configurations are as follows: (i) CO₂ molecule placed at site D1, parallel to MgO- $_O$ in such a way that (a) both O atoms of CO₂ are close to the Mg atom of MgO sheet (b) one O atom of CO₂ is facing the Mg atom and another facing an O atom of the MgO sheet, and (ii) a few perpendicular configurations, e.g. (a) at site D1 and (b) near site D1. The third configuration of **Figure S4** was found to be the most stable arrangement as it exhibits the maximum E_{ads} on MgO- $_O$ (-1.44 eV) (**Figure 3**). Comparing the interaction of CO₂ with the pristine 2D MgO sheet, we note that the E_{ads} and charge transfer of CO₂@MgO- $_O$ increases by 0.64 eV and 1.65 e⁻, respectively. This was expected as the loss of the oxygen atom produces electron abundant surroundings, which induce charge transfer interactions with CO₂ molecules. The band gap value changes from 1.20 eV to 1.29 eV as a result of interaction with CO₂ (**Figure 4**). Here, the CO₂ molecule bends with an angle of 119.58° and the C-O bond length stretches to 1.29 Å. As at adsorption site **D1**, there is a lack of a highly electronegative O-atom; therefore, the O atoms of the CO₂ molecules attract the electrons during the interaction with the MgO- $_O$ sheet and the CO₂ molecule becomes negatively charged.

Similar to various configurations tried at site D1 of MgO- $_O$, site D2 of the MgO- $_{Mg}$ sheet was also investigated for CO₂ activation. The relaxed structures of these configurations are shown in **Figure S5** of the supplementary file along with **Table S3**, which contains all adsorption and geometrical parameters. Among different configurations tested, the first configuration (see **Table S3**) was found to exhibit the largest E_{ads} value of -2.22 eV (**Figure 3**). Here, the CO₂ molecule acts as an electron donor while interacting with the MgO- $_{Mg}$ monolayer and gains a positive charge of 0.92e⁻ after activation (**Figure 5**). Moreover, significant reduction in the band gap was observed as the band gap reduces to 0.41 eV from its value of 2.24 eV (see **Figure 4**).

Next, we investigated the more porous MgO-Mg/O 2D sheet having both one Mg and one O atom vacancy. **Figure S6** shows the relaxed structures of different CO₂@ MgO-Mg/O systems, and their characteristic parameters are listed in **Table S4**. The most stable CO₂ configuration for the MgO-Mg/O system is found when one O atom of CO₂ was placed near the Mg atom of the MgO-Mg/O monolayer, and another O atom near site D3 with the C atom pointing to the O atom of the MgO-Mg/O system (first configuration of **Figure S6**), with a calculated E_{ads} energy of -3.97 eV (**Figure 3**) and a charge transfer of 0.12 e. Here, the CO₂ molecule loses electrons and becomes positively charged and thus more reactive towards nucleophiles like H⁻ from hydrogenation reactions, thereby enhancing its conversion. One can also note that the CO₂ adsorption energy value in this case is about five times higher than its value at the pristine 2D MgO sheet. The bond length and bond angle of the CO₂ molecule after activation on this sheet were 1.30 Å and 121.82°, respectively. A closer look at the PDOS and EBS indicates new sharp peaks near the Fermi level, resulting in a decrease of the energy gap to 0.17 eV.

Among anti-site defects, as mentioned, we only investigated the CO₂ molecule interaction on MgO-AO systems. We placed the CO₂ molecule in different orientations near the extra O atom (near site **D4**). As the O atom is highly electronegative, and three O atoms surround site D4, these atoms pull electrons during interaction with the CO₂ molecule which acts as an electron donor. The net charge on the CO₂ molecule at the MgO-AO system was 1.94 e⁻ (**Figure 5**) Here, the separation between the energy bands was found to be 1.40 eV (**Figure S3**). The summary and plots of all tested configurations of CO₂ molecules at the MgO-AO system are summarized in **Table S5** and **Figure S7** of the supplementary file.

We found MgO-O to be the most suitable 2D MgO sheet towards reducing CO₂ into valuable products (**Figure 5**), as strong chemisorption is observed for the CO₂ molecule. To confirm the thermodynamical favorability of CO₂ at various MgO systems, we also computed the Gibbs free energy of the CO₂ adsorbed systems. From **Table 2**, it is clear that $\Delta G < 0$ for all CO₂ adsorbed systems. Thus, the CO₂ adsorption process at MgO systems is spontaneous and strong enough to keep adsorbed CO₂ molecule bound for further electrochemical conversion.

The present study has focused on the thermodynamics of CO₂ activation at various 2D MgO sheets as the crucial first step in CO₂ conversion reactions. In order to obtain full reaction pathways in

the electrochemical conversion of CO₂ to chemicals and fuels will require the calculation of reaction kinetics, which will be the focus of future work.

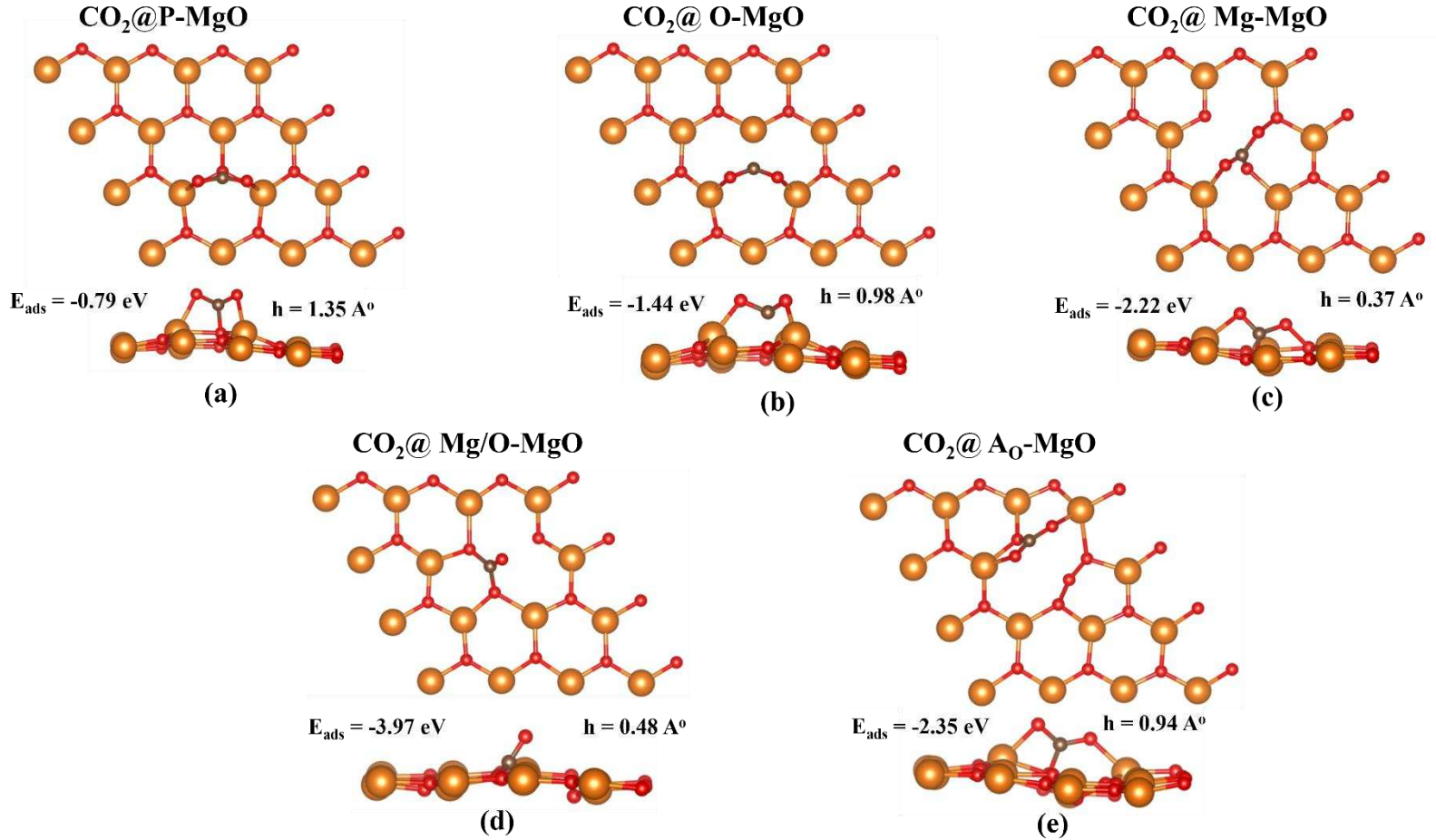


Fig. 3. Relaxed structures after CO₂ adsorption on (a) MgO, (b) MgO-O, (c) MgO-Mg, (d) MgO-Mg/O, and (e) MgO-AO sheets

Table 2

Calculated adsorption energy E_{ads} (eV), defect formation energy E_{def} (eV), Gibbs free energy ΔG (eV) adsorption height h (Å), bond lengths l (Å), bond angle θ (°), band gap E_g (eV) and charge transfer Δq_{CO_2} (e^-) of most stable CO₂ configurations on different 2D MgO sheets

System	E_{ads}	E_{def}	ΔG	h	l		θ	E_g	Δq_{CO_2}
					Mg-O	C-O			

MgO	-0.79	--	-0.83	1.35	2.15	1.26	130.51	2.29	-0.02
MgO-o	-1.44	-10.04	-1.49	0.98	1.89	1.29	119.58	1.29	-1.67
MgO-Mg	-2.22	-10.51	-2.29	0.37	1.91	1.31	113.46	0.41	0.94
MgO-Mg/O	-3.97	-16.87	-4.02	0.48	1.91	1.30	121.82	0.17	0.12
MgO-AO	-2.35	-5.65	-2.39	0.94	1.97	1.28	126.41	1.40	1.94

From the PDOS (**Figure 4**), it is clear that hybridization between the p-orbital of C and the s-orbital of Mg takes place, causing a sharp peak near -2.5 eV, while overlap of C(p) and O(p) orbitals is found near 1eV and -2eV, suggesting a strong interaction between CO₂ and the MgO-o sheet. Similar minor peaks of C(p) orbitals are observed near -2.5, -3 and -4 eV for CO₂ adsorbed at the MgO-Mg, MgO-Mg/O and MgO-Ao sheets. In contrast, when the CO₂ molecule interacts with defect-containing MgO (110) surfaces (Lv et al.)[16], bond formation between the Mg atom of MgO and the O atom of CO₂ takes place, mainly owing to the contribution of Mg(3s)-O(2p) and Mg(3s)-O(2s) orbital pairs.

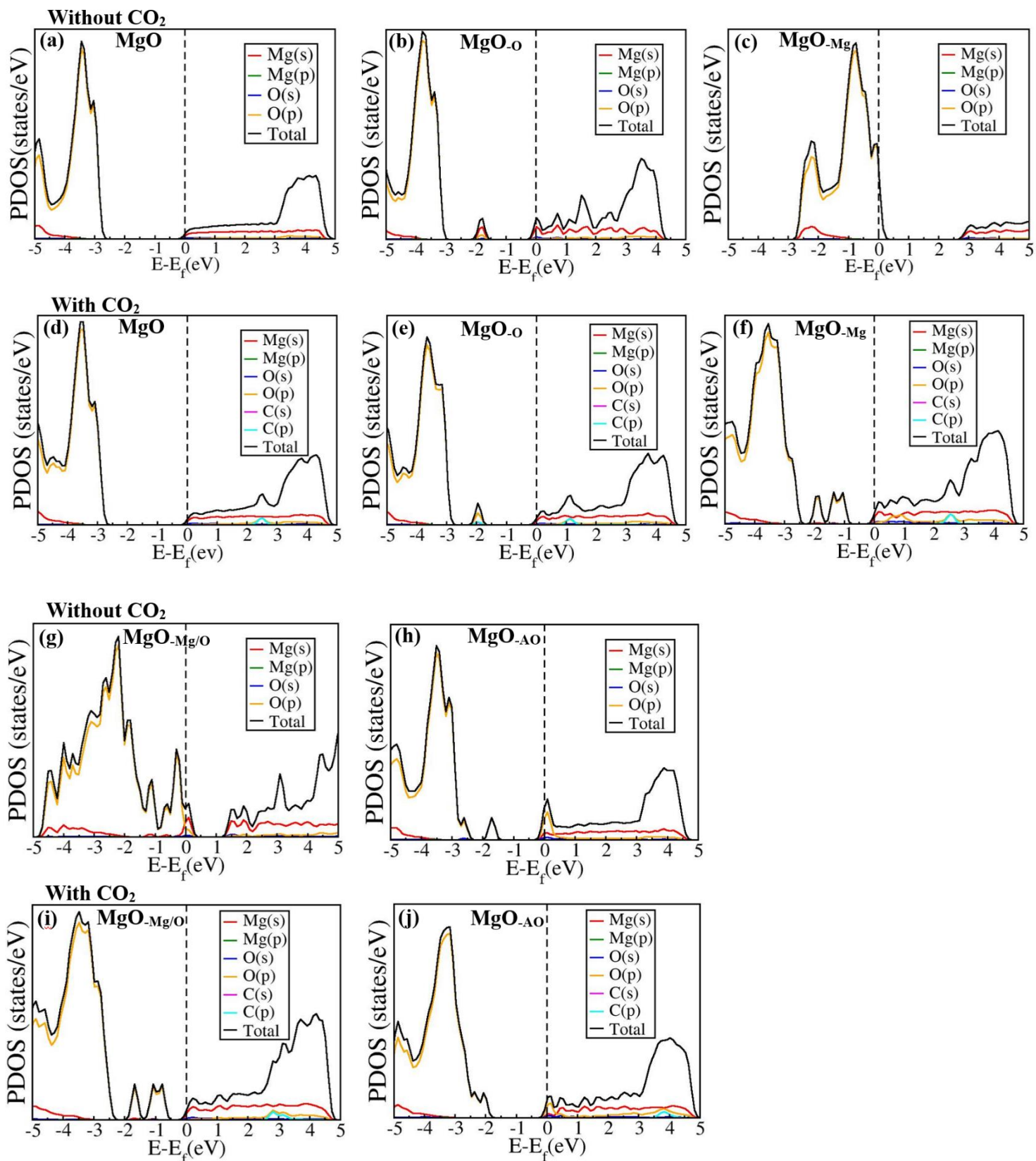


Fig. 4. PDOS plots of various MgO sheets before and after CO_2 adsorption.

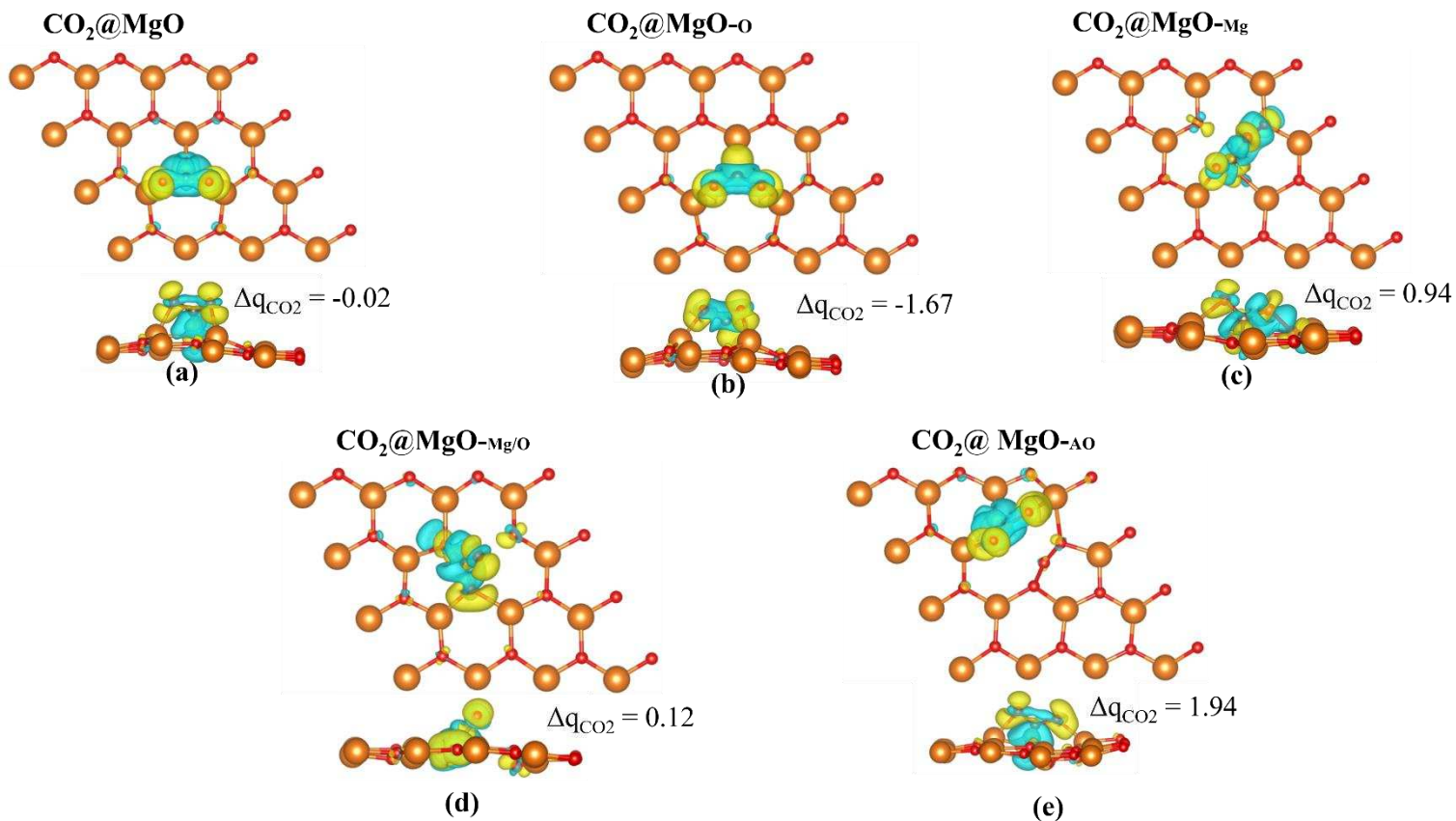


Fig. 5. Charge density difference plots after CO₂ adsorption on (a) MgO, (b) MgO-o, (c) MgO-Mg, (d) MgO-Mg/O, and (e) MgO-AO sheets

4. Conclusion

We have investigated various defect formations in a 2D MgO monolayer sheet. Our calculations indicate favourable atomic and molecular defect formations, while the MgO-AMg anti-site defect is found to be unfavourable. CO₂ molecule activation was investigated where it was found that the CO₂ molecule is chemically adsorbed with an adsorption energy of -0.79 eV and bends over the pristine 2D MgO monolayer sheet, while defects were found to further enhance the CO₂ activation. The creation of single O and Mg vacancies on 2D MgO increases the adsorption energy of CO₂ by about 80% and 178%, respectively. The maximum CO₂ adsorption energy was found at the MgO-Mg/O system (-3.97 eV) among all energetically stable systems. We conclude that CO₂ activation can be achieved and improved by engineering various atomic and molecular defects into a 2D MgO sheet. Our findings indicate that 2D MgO is a promising candidate for the electrochemical conversion of CO₂ into valuable chemicals and fuels.

Supplementary Information

We have provided all studied CO₂ on the pristine, and defect-containing 2D MgO sheets in the ESI. Fig. S1 contains the EBS of all 2D MgO sheets. Fig. S2 shows six relaxed configurations of CO₂ at pristine 2D MgO sheets. Fig S3 represents EBS of the most stable CO₂ configurations at pristine and defect-containing 2D MgO sheets. Fig S4-S7 represent adsorption of CO₂ at MgO-o, MgO-Mg, MgO-Mg/O and MgO-AO sheets, respectively. Table S1-S5 contain adsorption energies along with adsorption heights and relaxed bond lengths of CO₂ adsorbed at 2D MgO, MgO-o, MgO-Mg, MgO-Mg/O and MgO-AO sheets, respectively.

Acknowledgment

A.K.M. acknowledges the SERB SURE grant (SUR/2022/004935-year 2023) and SEED 2021 grant from UPES for computational facilities. Via our membership of the UK's HEC Materials Chemistry Consortium, which is funded by EPSRC (EP/X035859), we also acknowledge the use of the ARCHER2 UK National Supercomputing Service (<https://www.archer2.ac.uk>).

References

- [1] P. Kumbhakar, C. Chowde Gowda, P.L. Mahapatra, M. Mukherjee, K.D. Malviya, M. Chaker, A. Chandra, B. Lahiri, P.M. Ajayan, D. Jariwala, A. Singh, C.S. Tiwary, Emerging 2D metal oxides and their applications, *Materials Today* 45 (2021) 142–168. <https://doi.org/10.1016/j.mattod.2020.11.023>.
- [2] K. Zhou, G. Shang, H.H. Hsu, S.T. Han, V.A.L. Roy, Y. Zhou, Emerging 2D Metal Oxides: From Synthesis to Device Integration, *Advanced Materials* 35 (2023) 2207774. <https://doi.org/10.1002/adma.202207774>.
- [3] H. Zheng, X. Bin Li, N.K. Chen, S.Y. Xie, W.Q. Tian, Y. Chen, H. Xia, S.B. Zhang, H.B. Sun, Monolayer II-VI semiconductors: A first-principles prediction, *Phys Rev B Condens Matter Mater Phys* 92 (2015) 115307. <https://doi.org/10.1103/PhysRevB.92.115307>.
- [4] S. Ahmed, A. Iqbal, Synthesis of 2D Magnesium Oxide Nanosheets: A Potential Material for Phosphate Removal, *Global Challenges* 2 (2018) 1800056. <https://doi.org/10.1002/gch2.201800056>.
- [5] D.M. Hoat, V. Van On, D.K. Nguyen, M. Naseri, R. Ponce-Pérez, T. V. Vu, J.F. Rivas-Silva, N.N. Hieu, G.H. Cocolletzi, Structural, electronic and optical properties of pristine and functionalized MgO monolayers: A first principles study, *RSC Adv* 10 (2020) 40411–40420. <https://doi.org/10.1039/d0ra05030j>.

- [6] A.D. Moghadam, P. Maskane, S. Esfandiari, Electronic, magnetic and optical properties of B, C, N and F doped MgO monolayer, *Physica C: Superconductivity and Its Applications* 549 (2018) 33–36. <https://doi.org/10.1016/j.physc.2018.02.059>.
- [7] S. Pavithra, B. Mohana, M. Mani, P.E. Saranya, R. Jayavel, D. Prabu, S. Kumaresan, Bioengineered 2D Ultrathin Sharp-Edged MgO Nanosheets Using *Achyranthes aspera* Leaf Extract for Antimicrobial Applications, *J Inorg Organomet Polym Mater* 31 (2021) 1120–1133. <https://doi.org/10.1007/s10904-020-01772-7>.
- [8] J.I. Di Cosimo, V.K. Díez, C. Ferretti, C.R. Apesteguía, Basic catalysis on MgO: Generation, characterization and catalytic properties of active sites, *Catalysis* 26 (2014) 1–28. <https://doi.org/10.1039/9781782620037-00001>.
- [9] V.K. Díez, C.R. Apesteguía, J.I. Di Cosimo, Acid-base properties and active site requirements for elimination reactions on alkali-promoted MgO catalysts, *Catalysis Today* 63 (2000) 53–62. [https://doi.org/10.1016/S0920-5861\(00\)00445-4](https://doi.org/10.1016/S0920-5861(00)00445-4)
- [10] S. Balu, A. Hanan, H. Venkatesvaran, S.-W. Chen, T.C.-K. Yang, M. Khalid, Recent Progress in Surface-Defect Engineering Strategies for Electrocatalysts toward Electrochemical CO₂ Reduction: A Review, *Catalysts* 13 (2023) 393. <https://doi.org/10.3390/catal13020393>.
- [11] S.S.A. Shah, M. Sufyan Javed, T. Najam, C. Molochas, N.A. Khan, M.A. Nazir, M. Xu, P. Tsiakaras, S.-J. Bao, Metal oxides for the electrocatalytic reduction of carbon dioxide: Mechanism of active sites, composites, interface and defect engineering strategies, *Coord Chem Rev* 471 (2022) 214716. <https://doi.org/10.1016/j.ccr.2022.214716>.
- [12] R. Daiyan, E.C. Lovell, N.M. Bedford, W.H. Saputera, K. Wu, S. Lim, J. Horlyck, Y.H. Ng, X. Lu, R. Amal, Modulating Activity through Defect Engineering of Tin Oxides for Electrochemical CO₂ Reduction, *Advanced Science* 6 (2019) 1900678. <https://doi.org/10.1002/advs.201900678>.
- [13] E. Scorza, U. Birkenheuer, C. Pisani, The oxygen vacancy at the surface and in bulk MgO: An embedded-cluster study, *J Chem Phys* 107 (1997) 9645–9658. <https://doi.org/10.1063/1.475260>.
- [14] L. Ojamäe, C. Pisani, Theoretical characterization of divacancies at the surface and in bulk MgO, *J Chem Phys* 109 (1998) 10984–10995. <https://doi.org/10.1063/1.477793>.
- [15] P. Baranek, G. Pinarello, C. Pisani, R. Dovesi, Ab initio study of the cation vacancy at the surface and in bulk MgO, *Physical Chemistry Chemical Physics* 2 (2000) 3893–3901. <https://doi.org/10.1039/B003590O>.
- [16] G. Lv, C. Zhu, H. Zhang, Y. Su, P. Qian, Mechanism of CO₂ adsorption on point-defective MgO surfaces: First-principles study, *Appl Surf Sci* 604 (2022) 154647. <https://doi.org/10.1016/j.apsusc.2022.154647>.
- [17] D. Cornu, H. Guesmi, J.-M. Krafft, H. Lauron-Pernot, H. Lauron, Lewis acido-basic interactions between CO₂ and MgO surface: DFT and DRIFT approaches Lewis acido-basic interactions

- between CO₂ and MgO surface: DFT and DRIFT approaches, *Journal of Physical Chemistry C* 116 (2012)6645-6654. <https://doi.org/10.1021/jp211171ti>.
- [18] J.P. Singh, V. Singh, A. Sharma, G. Pandey, K.H. Chae, S. Lee, Approaches to synthesize MgO nanostructures for diverse applications, *Heliyon* 6 (2020) e04882. <https://doi.org/10.1016/j.heliyon.2020.e04882>.
- [19] V. Van On, J. Guerrero-Sanchez, R. Ponce-Pérez, T. V. Vu, J.F. Rivas-Silva, G.H. Coccoletzi, D.M. Hoat, Defective and doped MgO monolayer as promising 2D materials for optoelectronic and spintronic applications, *Mater Sci Semicond Process* 149 (2022) 106876. <https://doi.org/10.1016/j.mssp.2022.106876>.
- [20] R. Hazarika, B. Kalita, Effect of oxygen vacancy defects on electronic and optical properties of MgO monolayers: First principles study, *Materials Science and Engineering: B* 286 (2022) 115974. <https://doi.org/10.1016/j.mseb.2022.115974>.
- [21] P. Giannozzi, O. Andreussi, T. Brumme, O. Bunau, M.B. Nardelli, M. Calandra, R. Car, C. Cavazzoni, D. Ceresoli, M. Cococcioni, N. Colonna, I. Carnimeo, A. Dal Corso, S. De Gironcoli, P. Delugas, R.A. Distasio, A. Ferretti, A. Floris, G. Fratesi, G. Fugallo, R. Gebauer, U. Gerstmann, F. Giustino, T. Gorni, J. Jia, M. Kawamura, H.-Y. Ko, A. Kokalj, E. Küçükbenli, M. Lazzeri, M. Marsili, N. Marzari, F. Mauri, N.L. Nguyen, H.-V. Nguyen, A. Otero-De-La-Roza, L. Paulatto, S. Poncé, D. Rocca, R. Sabatini, B. Santra, M. Schlipf, A.P. Seitsonen, A. Smogunov, I. Timrov, T. Thonhauser, P. Umari, N. Vast, X. Wu, S. Baroni, Advanced capabilities for materials modelling with Quantum ESPRESSO, *Journal of Physics: Condensed Matter* 29 (2017) 465901. <https://doi.org/10.1088/1361-648X/aa8f79>
- [22] G.K.H. Madsen, Functional form of the generalized gradient approximation for exchange: The PBE α functional, *75* (2006) 195108. <https://doi.org/10.1103/PhysRevB.75.195108>
- [23] J.P. Perdew, K. Burke, M. Ernzerhof, Generalized Gradient Approximation Made Simple, *Physical Reviews Letters*, *77* (1996) 3865. <https://doi.org/10.1103/PhysRevLett.77.3865>
- [24] P.E. Blöchl, Projector-Augmented Wave Method: ab-initio MD with full wave functions, *Physical Review B* 24(2002) 17953. <http://www.pt.tu-clausthal.de/atp/>.
- [25] E. Caldeweyher, S. Ehlert, A. Hansen, H. Neugebauer, S. Spicher, C. Bannwarth, S. Grimme, A generally applicable atomic-charge dependent London dispersion correction, *The Journal of chemical Physics* 150 (2019) 154122. <https://doi.org/10.1063/1.5090222>
- [26] V. Van On, J. Guerrero-Sanchez, R. Ponce-Pérez, T. V. Vu, J.F. Rivas-Silva, G.H. Coccoletzi, D.M. Hoat, Defective and doped MgO monolayer as promising 2D materials for optoelectronic and spintronic applications, *Mater Sci Semicond Process* 149 (2022) 106876. <https://doi.org/10.1016/j.mssp.2022.106876>.
- [27] M.M. Alyörük, Piezoelectric properties of monolayer II–VI group oxides by first-principles calculations, *Phys Status Solidi B Basic Res* 253 (2016) 2534–2539. <https://doi.org/10.1002/pssb.201600387>.

- [28] A. Bafekry, M. Faraji, S. Karbasizadeh, A.B. Khatibani, A.A. Ziabari, D. Gogova, M. Ghergherehchi, Point defects in two-dimensional BeO monolayer: a first-principles study on electronic and magnetic properties, *Physical Chemistry Chemical Physics* 23 (2021) 24301–24312. <https://doi.org/10.1039/d1cp03421a>.
- [29] J. Zhu, A. Chroneos, U. Schwingenschlögl, CO₂ capture by Li-functionalized silicene, *Physica Status Solidi - Rapid Research Letters* 10 (2016) 458–461. <https://doi.org/10.1002/pssr.201600102>.
- [30] C. Wang, Y. Fang, H. Duan, G. Liang, W. Li, D. Chen, M. Long, DFT study of CO₂ adsorption properties on pristine, vacancy and doped graphenes, *Solid State Commun* 337 (2021) 114436. <https://doi.org/10.1016/j.ssc.2021.114436>.